THE EFFECTS OF PERIODICALLY GAPPED TIME SERIES ON CROSS-CORRELATION LAG DETERMINATIONS

Y.H. Zhang

Center for Astrophysics, Department of Physics, Tsinghua University, 100084 Beijing, P.R. China, and Dipartimento di Scienze, Università degli Studi dell'Insubria, via Valleggio 11, I-22100 Como, Italy

youhong.zhang@mail.tsinghua.edu.cn; youhong.zhang@uninsubria.it

I. Cagnoni, A. Treves

Dipartimento di Scienze, Università degli Studi dell'Insubria, via Valleggio 11, I-22100 Como, Italy

A. Celotti

International School for Advanced Studies, SISSA/ISAS, via Beirut 2-4, I-34014 Trieste, Italy

L. Maraschi

Osservatorio Astronomico di Brera, via Brera 28, I-20121 Milano, Italy

ABSTRACT

The three bright TeV blazars Mrk 421, Mrk 501 and PKS 2155–404 are highly variable in synchrotron X-ray emission. In particular, these sources may exhibit variable time lags between flux variations at different X-ray energy bands. However, there are a number of issues that may significantly bias lag determinations. Edelson et al. (2001) recently proposed that the lags on timescales of hours, discovered by *ASCA* and *BeppoSAX*, could be an artifact of periodic gaps in the light curves introduced by the Earth occultation every ~ 1.6 hr. Using Monte Carlo simulations, in this paper we show that the lags over timescales of hours can not be the spurious result of periodic gaps, while periodic gaps indeed introduces uncertainty larger than what present in the evenly sampled data. The results also show that time lag estimates can be substantially improved by using evenly sampled light curves with large lag to bin-size ratio. Furthermore, we consider an *XMM-Newton* observation without interruptions and re-sample the light curves using the *BeppoSAX* observing windows, and then repeat the same

cross correlation function (CCF) analysis on both the real and fake data. The results also show that periodic gaps in the light curves do not significantly distort the CCF characters, and indeed the CCF peak ranges of the real and fake data overlap. Therefore, the lags discovered by *ASCA* and *BeppoSAX* are not due to periodic gaps in the light curves.

Subject headings: BL Lacertae objects: general — galaxy: active — galaxy: nuclei — numerical methods — X-rays: galaxy

1. Introduction

One of the main advances from recent X-ray observations of blazars is the discovery of the energy-dependent time lags in the X-ray emission of the three bright TeV-emitting blazars Mrk 421, Mrk 501 and PKS 2155–304. The overall spectral energy distributions (SEDs) show that the synchrotron emission component from these sources peaks at high-energy (UV/soft X-ray) band. This indicates that the X-ray emission from these sources is the high energy tail of the synchrotron component, where the most violent variability is expected. The inter-band time lag is one of the important variability parameters. The cross-correlation function (CCF) technique is the standard tool for lag determinations. *ASCA* and *BeppoSAX* discovered that in these sources the lower energy X-ray photons may lag or lead the higher energy ones, i.e., the so-called soft or hard lag, respectively. The signs and values of the lags may well depend on either energy or on the single flare analyzed. The typical lags (either soft or hard lag) range from $\sim$ zero to 10^4 s (see Zhang et al. 2002 for a review), and appear to be correlated to the flare duration: the shorter the flare duration, the smaller the lag (Zhang et al 2002; Brinkmann et al. 2003). Zhang (2002) also found evidence for a dependence of lags on timescales in Mrk 421: lags appear to be larger on longer timescales. The observed lags have been interpreted as evidence for the interplay of the acceleration and cooling timescales of relativistic electrons responsible for the observed X-rays taking place in the jets (e.g., Kirk, Rieger & Mastichiadis 1998), and used to constrain the main parameters of the emitting region on the basis of variability (e.g., Zhang et al. 2002) rather than of SEDs, as commonly used.

However, the latest lag searches with *XMM-Newton* have put the discovery of *ASCA* and *BeppoSAX* into question. Edelson et al. (2001) and Sembay et al. (2002) reported that there is no evidence for measurable inter-band lags in the X-rays, with upper limits of $\sim$ 0.3 (PKS 2155–304) and 0.08 hr (Mrk 421). It is commonly believed that uninterrupted time series, due to the highly eccentric $\sim$ 48 hours orbit of *XMM-Newton*, allow to detect more reliably the lags. This has led these authors to propose that the lags measured with

ASCA and *BeppoSAX* could well be an artifact of the periodic interruptions by the Earth occultation related to the short *ASCA* and *BeppoSAX* orbital period ($\sim$ 1.6 hr). Maraschi et al. (2002) also reported no measurable lags with a full orbit *XMM-Newton* observation of PKS 2155–304. Brinkmann et al. (2003) re-analyzed all the available *XMM-Newton* observations of Mrk 421, working with light curves that have a small bin-size of 8 s, and found typical lags of $\sim$ 5 min.

In order to address the issue of the reliability and significance of the lags discovered by *ASCA* and *BeppoSAX*, in this paper we perform Monte Carlo simulations to investigate the effects of periodically gapped time series on CCF lag determinations. A number of simulations using inverse Fourier transformation, which is model-dependent, have been carried out in the literature to evaluate the significance and uncertainty of the CCF lag determinations either for poorly sampled time series (e.g., Gaskell & Peterson 1987; Maoz & Netzer 1989; White & Peterson 1994) or for evenly sampled time series (e.g., Welsh 1999). The issue of poorly irregular sampling and noisy data was also previously investigated (see the summary in Koen 1994). There are a number of issues that can significantly bias the reliability of CCF lag determinations. We refer to Welsh (1999) for a review on such issue, where the author also showed the effects of power spectral density (PSD) slope, duration, signal-to-noise ratio, de-trending and tapering of light curves. We note, however, that the previous simulations mainly dealt with the relationship between the UV/optical emission line flux and the continuum variations in Seyfert galaxies, which applied to the reverberation mapping (to measure the size of broad-line region) and typical ground-based irregular sampling patterns. In the blazar context, the simulations by Litchfield, Robson, & Hughes (1995) were performed on the radio sampling patterns. Our simulations are tailored to match the sampling characteristics of space-based observations introduced by low earth orbit satellites, which to our knowledge have not been explicitly addressed in astronomical literature. Another distinction is that we discuss the time lags between the variations of the synchrotron emission in different X-ray bands. In particular, it is worth noting that there are obvious difficulties in accurately determining lags in the synchrotron X-ray emission of TeV blazars as (1) the lags are short compared to the bin-sizes of the available data; (2) the data are usually not equally sampled – in particular periodical interruptions of space-based observations are unavoidable for the low Earth orbit satellites; and (3) there are ambiguities in interpreting the complexities of the CCF results.

In this work we also make use of the method introduced by Peterson et al. (1998), namely a model-independent Monte Carlo method to assess the uncertainties in the lag measurements obtained. This method does make use of real data, and is known as flux redistribution/random subset selection (FR/RSS) that is based on the "bootstrap" method. Here we adopt it to study the effects of periodic gaps in lag determinations. To do so, we

use a real *XMM-Newton* observation without interruptions, and re-sample it with the typical *BeppoSAX* sampling windows. The same CCF analysis is then performed on both the real and fake time series.

In §2 we conduct model-dependent simulations: §2.1 illustrates the assumptions for the simulations to be performed; and the results are presented in §2.2. The model-independent simulations are performed in §3. We discuss the significance of our results in §4.

2. Monte Carlo Simulations

2.1. Assumptions

The inverse Fourier transformation from frequency to time domain is usually performed to simulate light curves by assuming a PSD model. We use the algorithm of Timmer & König (1995), which randomizes both the amplitude and the phase of a red noise process at each Fourier frequency. In exploring the full variety of possible light curves showing the same PSD, this algorithm is superior to the commonly used one that randomizes phases only (Benlloch et al. 2001; Uttley, M$^{\rm c}$Hardy, & Papadakis 2002). In order to mimic a real situation as closely as possible, we normalize fake light curves on the basis of the real variability behavior of one observation of Mrk 421 obtained with *BeppoSAX* (Fossati et al. 2000; Zhang 2002) as this observation has a good signal-to-noise ratio that will lay stress on the key point of this investigation. The assumptions and procedure of our simulations are as follows.

A simple power-law PSD, i.e., $P(f) \propto f^{-\alpha}$ with slope $\alpha = 2.5$ is assumed (Zhang 2002) to represent the red noise variability of the bright TeV blazars (Kataoka et al. 2001; Zhang et al. 1999; 2002), and from this the light curves are recovered on the basis of Monte Carlo technique. With one set of Gaussian distributed random numbers, we construct a fake pair of light curves that evenly sample 171 points with bin-size $\Delta t = 512$ s. This choice resembles the binned light curves of Mrk 421 used in Zhang (2002) to perform the CCF analysis. At the same time, in order to mimic the discovered time lags, we delay the phase of the second light curve of the fake pair on the basis of the relationship $\Delta\phi(f_i) = 2\pi f_i \tau(f_i)$, where f_i is the Fourier frequency ($i = 1, ..., N/2$; $N = 171$ is the total number of the evenly sampled light curve points), $\tau(f_i)$ is the time lag and $\Delta\phi(f_i)$ the phase lag at f_i. For simplicity, we assume that τ is frequency-independent, i.e., $\tau =$ constant (see, however, Zhang 2002 for the evidence of the dependence of τ on frequency), and in turn $\Delta\phi(f_i) = 2\pi\tau f_i$. An assumed (true) lag τ therefore corresponds to the lag determined with the CCF methods. The aim of our simulations is to recover the assumed τ by applying the CCF methods to the fake pair

with specific sampling windows. The two light curves of the fake pair are then scaled to have the same mean and variance as the real 0.1–2 keV and 2–10 keV light curves of Mrk 421 (Zhang 2002), respectively. In order to mimic photon counting (Poisson) white noise, the two fake light curves are further Gaussian randomly redistributed on the basis of the average errors on the real 0.1–2 keV and 2–10 keV light curves of Mrk 421. In order to simulate the periodic gaps of the light curves obtained with *BeppoSAX*, we re-sample the two fake light curves by applying the real observing windows on the 0.1–2 keV and 2–10 keV light curves of Mrk 421. Three CCF methods, i.e., interpolation cross correlation function (ICCF, White & Peterson 1994), Discrete Correlation Function (DCF, Edelson & Krolik 1998), and *Fisher's z-transformed* DCF (ZDCF, Alexander 1997) that is based on the DCF, are then used to cross-correlate the two fake light curves before and after applying the real observing windows. All CCFs are normalized by the mean and standard deviation of the two cross-correlated light curves using only the data points that actually contribute to the calculation of each lag (White & Peterson 1994), since the light curves in our cases are not stationary. A simulation is deemed to have succeeded if $r_{\rm max}$ (the maximum value of the CCF) between the two fake light curves is significant at a level of confidence greater than 95% (Peterson et al. 1998). For each succeeded trial, we record the lags using three techniques to interpret the CCF results: (1) using the lag corresponding to $r_{\rm max}$ of the CCF, $\tau_{\rm peak}$; (2) computing the centroid of the CCF over time lags bracketing $r_{\rm max}$, $\tau_{\rm cent}$ – all the CCF points with r in excess of $0.8r_{\rm max}$ are used (Peterson et al. 1998); (3) fitting the CCF with a Gaussian function to find the location of the CCF peak, $\tau_{\rm fit}$. We repeat this procedure 2000 times to construct probability distributions of the lags (i.e., the cross-correlation peak distribution, CCPD; Maoz & Netzer 1989) for $\tau_{\rm peak}$, $\tau_{\rm cent}$, and $\tau_{\rm fit}$.

2.2. Results

We simulate time lags covering the range discovered by ASCA and *BeppoSAX* in TeV blazars. Therefore, we arbitrarily assume $\tau = 0, 300, 1400, 3000, 5400, 7100$ s, respectively. We create fake light curves using the same sets of random number for each case except for different τ.

Figure 1a, as an example, shows a pair of fake light curves that are evenly sampled, and the second light curve (solid circles) is delayed by $\tau = 3000$ s with respect to the first one (open circles). The lag is clearly visible by comparing both the peaks and the troughs of the two light curves. In this case, the ratio of τ to Δt of the light curves is ~ 6. The ICCF, DCF and ZDCF of the two light curves are shown in Figure 1b-d (solid lines). We use $\tau_{\rm peak}$, $\tau_{\rm cent}$, and $\tau_{\rm fit}$ to measure the lag, respectively. The results are reported in Table 1. One

can see that the true lag is properly recovered by the different CCF methods and different techniques used to interpret the CCFs.

We then re-sample these two light curves using the real *BeppoSAX* observing windows as mentioned in §2.1. The resulted light curves thus are affected by periodic gaps resembling the light curves obtained with *BeppoSAX*. Note that the number of points (63) in the first re-sampled light curve is smaller than that in the second one (76) because on-board *BeppoSAX* the LECS detector is less exposed than the MECS one. The ICCF, DCF and ZDCF of the two light curves with periodic interruptions are shown in Figure 1b-d (dotted line or open circles with error bars). The measured lags are also reported in Table 1. In this case, both $\tau_{\rm peak}$ and $\tau_{\rm cent}$ underestimate the true lag while $\tau_{\rm fit}$ of the DCF and ZDCF still recover it, although with larger uncertainties. Figure 1b-d also show that the overall characteristics of the CCFs obtained from the evenly sampled light curves are almost identical to those obtained from the corresponding light curves with periodic gaps. However, due to the missing of a large number of data points in the latter case, the CCF peaks somewhat shift to smaller lags. Note that $\tau_{\rm fit}$ is not calculated for the ICCF case because there are no estimates of the ICCF errors, and the DCF errors are overestimated with respect to the ZDCF ones.

The statistical significance of the effects of periodic gaps on the CCF lag determinations is deduced from the probability distributions of a number of simulations. We show in Figure 2 (ICCF), Figure 3 (DCF), and Figure 4 (ZDCF) the CCPDs of the simulated lags for the case $\tau = 0$ and 3000 s. It is worth noting that the CCPDs are almost always non-normal distributions, in particular for $\tau_{\rm peak}$ and $\tau_{\rm cent}$. Therefore, we use the median and 68% confidence level (with respect to the median) to statistically characterize the CCPDs. The statistical results for all the simulations performed are tabulated in Table 2. The first column is the assumed true lag, and columns 2–4 and 5–7 give the CCPD median and 68% confidence range for evenly sampled and periodically gapped light curves, respectively. As shown in Figures 2-4 and Table 2, the main results of our simulations can be summarized as follows: (1) the assumed true lags are recovered in all cases in terms of the CCPD medians with 68% confidence errors; (2) the main effect of periodic gaps is to broaden the CCPDs, thus to increase the uncertainty of the CCF lag determinations. Most importantly, periodic gaps do not produce artificial CCF lags. More specifically, from the simulations with true small lags (e.g, the cases of 0 and 300 s lags), one can see that periodic interruptions in the light curves definitely do not produce spurious lags on timescales of hours; (3) in some cases, the three CCF methods and the three techniques used to interpret the CCF results do not give rise to completely consistent results. For example, $\tau_{\rm peak}$ strongly depends on the lag steps used to calculate the CCF; the errors of the DCF are overestimated, thus producing the broadest CCPDs.

These results imply that (1) evenly sampled light curves with large lag to bin-size ratios give more reliable CCF lag determinations; (2) more importantly, the lags on timescales of hours discovered by *ASCA* and *BeppoSAX* can not be an artifact of periodic gaps in the light curves that have intrinsically small lag; (3) the only effect of periodic gaps is to introduce uncertainty and to increase the variance on the CCF lag determinations.

3. A Specific Case: *XMM-Newton* Observations of PKS 2155–304

The simulations presented in the previous section showed that periodical gaps in the light curves do not produce spurious lags between them, but only increase the uncertainty and variance in lag determinations. Uninterrupted data with high temporal resolution are available from *XMM-Newton* observations of Mrk 421 and PKS 2155–304. All of the CCF analysis, performed by Brinkmann et al. (2001; 2003), Edelson et al. (2001), Sembay et al. (2002), and Maraschi et al. (2002) showed that the inter-band lags between the soft and hard energy band are close to zero, with upper limits of about 1000 s. As we pointed out in the Introduction, these results led Edelson et al. (2001) to suggest that previous claims of time lags on time scales of hours might be an artifact of the periodic interruptions every $\sim$1.6 hours due to the low-Earth orbits of satellites such as *ASCA* and *BeppoSAX*. Therefore, in addition to the simulations presented in the previous section arguing against the above suggestion, an important test to assess the role of periodic gaps is to consider the *XMM-Newton* data and re-sample them according to the *ASCA* or *BeppoSAX* observing windows, and then repeat the CCF analysis on the fake *ASCA* or *BeppoSAX* data. Whether or not inter-band lags would be detected from the fake data would be a strong argument in favor or against the claim by Edelson et al. (2001).

In order to perform such a test, we take the first part of the *XMM-Newton* observation of PKS 2155–304 (Maraschi et al. 2002). The details of the data reduction and CCF analysis will be presented in Maraschi et al. (in preparation). For our purposes we just extracted the light curves in two energy bands, i.e., 0.7-1 and 1-2 keV. The light curves (without interruptions) are shown in Figure 5a. First, we performed the CCF analysis on them: the results are shown in Figure 5b-d (solid line) for the ICCF, DCF and ZDCF, respectively. We then re-sampled the light curves with the typical *BeppoSAX* sampling windows, obtaining two light curves with periodic interruptions resembling real *BeppoSAX* observations. We performed the same CCF analysis on the fake light curves with periodic gaps just as we did on light curves without gaps. The results are also shown in Figure 5b-d (dotted line or open circles with error bars). In all cases the two light curves are highly correlated near zero lag, and the CCFs calculated from the real and fake data overlap near their peaks, suggesting

that the periodic interruptions do not change the CCF character near the peak. We also measured the lags with the three techniques. The results are tabulated in Table 3. Due to the complexities of the CCFs, the measured lags depend on the CCF methods and the techniques used to quantify the CCFs. However, the results show in general that the real lag may be close to zero, with 0.7-1 keV photons very marginally leading the 1-2 keV photons.

Finally, we performed FR simulations (i.e., Gaussian randomly redistributing the light curves on the basis of the quoted errors). The resulting CCPDs are shown in Figure 6. We used the same statistical method as we did in § 2.2 to characterize the CCPDs. The statistical results are tabulated in Table 4. Within the 68% confidence errors, $\tau_{\rm peak}$ gives lags consistent with zero, while $\tau_{\rm cent}$ and $\tau_{\rm fit}$ suggest positive lags of ∼1000–2000 s, but at a low confidence ($\sim 2\sigma$). Note that the low confidence of the lag detections may be caused by the complexities of the variability behavior and the dependence of variations on the energy band considered. This also explains the fact that different methods and techniques may give rise to inconsistent results. In any case the comparison of the results obtained – using the same method and technique – from the light curves with periodic gaps and without gaps does not favor the suggestion that the periodic interruptions may produce spurious lags.

4. Discussion and Conclusions

We performed two sets of simulations to investigate the effects of space-based observations with short orbital period ($\sim$ 1.6 hr) on the reliability and significance of CCF lag determinations, specifically for the energy-dependent variations of synchrotron X-ray emission of TeV blazars. The first set of simulations (§2) make use of fake light curves generated with the Fourier transformation method. We investigated two main issues: (1) the effects of periodic data gaps in the light curves; and (2) the effects of different lag to bin-size ratios of light curves. The simulations showed that evenly sampled light curves indeed yield more reliable CCF lags, with smaller variance, than the periodically gapped light curves do. However, the CCPD analysis clearly showed that the light curves with periodic gaps still preserve the nature of the true lags (regardless of the values) even though they introduce larger lag variances than the light curves without gaps. Moreover, larger ratio of lag to light curve bin-size can improve the significance of CCF lag determination. The second set of simulations is based on a real *XMM-Newton* observation without interruptions. We re-sampled it with the typical *BeppoSAX* sampling windows in order to study whether or not periodic interruptions may give rise to strong biases in CCF lag determinations. The complex nature of the variability in TeV blazars results in obvious difficulties when quantifying lags, and it is likely to be the source of discrepancies between the results quantified with different

techniques. However, the comparison of the results derived with the same CCF method and the same quantifying technique, shows that the light curves with periodic interruptions do not produce spurious lags on timescales of hours if their intrinsic lag is indeed small. Therefore, our investigations argue against the proposal by Edelson et al. (2001) that the lags of about an hour discovered by *ASCA* and *BeppoSAX* are an artifact of periodic gaps introduced by low Earth orbit satellites. We thus conclude that the lags discovered by *ASCA* and *BeppoSAX* are most likely due to intrinsic variability properties of the sources, and not artificially produced from an intrinsic zero lag by periodic gaps. However, due to the complexities of variability that produces complicated CCF – irregularities and complexities of CCF could well be caused by different properties of variability on different timescales (Zhang 2002) – it is not easy to quantify real lags with the CCF method and different CCF methods and interpreting techniques may work for different cases. Our simulations also confirm that uninterrupted light curves with large lag to bin-size ratios can improve accuracy of lag determinations, in particular for small lags that require high sampling rates of light curves.

Welsh (1999) showed that the reality of CCF lag determinations also depend (1) on the light curve auto-correlation function (ACF) sharpness (the sharper the ACFs, the narrower the CCF peak and the smaller the lag bias) and (2) on the ratio of the intrinsic lag to the duration of the light curves. The first dependence can be easily explained by recalling that a CCF is a convolution of two ACFs. The ACF sharpness is determined by the PSD steepness (the steeper the PSD, the broader the ACF). The X-ray PSDs of the three TeV blazars are steep (with slopes of $\sim$ 2–3; Kataoka et al. 2001; Zhang et al. 1999; 2002), the ACF and the CCF peaks are therefore broad. De-trending light curves might remove such bias, but it also removes the low-(Fourier) frequency variability of the sources. This can introduce serious errors into time series and needs to be done very carefully. The second dependence becomes important only for the lengths of light curves shorter than $\sim$ 4 times the lag, which is never the case for the TeV blazars observed in the X-rays (typical ratios of the lengths of light curves to lags are 10–100).

Finally, we stress that the real light curves of the bright TeV blazars are very complex (e.g., the relationship between light curves at different energies may not be represented by just one "fixed" lag). Such complexities definitely result in irregular CCF, e.g., the CCF peaks at zero lag but shows asymmetry, which makes the CCF methods less straightforward to lag determinations. The cross-spectral technique, a more complex tool used to determine the Fourier frequency-dependent lags, may have the advantage of avoiding such ambiguities at least over long timescales (see Zhang 2002 for details). However, because this method relies on the Fourier transformation, it is not applicable to unevenly spaced data. On the contrary, in time domain one can use the DCF to substitute the classical CCF when dealing with irregular data.

We thank the anonymous referee for constructive comments. This research has made use of the standard on-line archive provided by the *BeppoSAX* Science Data Center (SDC). This work is partly based on an observation with *XMM-Newton*, an ESA science mission. The Italian MIUR is acknowledged for financial support. The project is sponsored by the Scientific Research Foundation for the Returned Overseas Chinese Scholars, State Education Ministry.

REFERENCES

Alexander, T. 1997, in Astronomical Time Series, eds. D. Maoz, A. Sternberg and E.M. Leibowitz (Dordrecht:Kluwer), p.163

Benlloch, S., Wilms, J., Edelson, R., Yaqoob, T., & Staubert, R. 2001, ApJ, 562, L121

Brinkmann, W., Sembay, S., Griffiths, R. G., Branduardi-Raymont, G., Gliozzi, M., Boller, Th., Tiengo, A., Molendi, S., & Zane, S. 2001, A&A, 356, L162

Brinkmann, W., Papadakis, I.E., den Herder, J.W.A., & Haberl, F. 2003, A&A, 402, 929

Edelson, R. A., & Krolik, J. H. 1988, ApJ, 333, 646

Edelson, R. A., Griffiths, G., Markowitz, A., Sembay, S., Turner, M. J. L., & Warwick, R. 2001, ApJ, 554, 274

Fossati, G., et al. 2000, ApJ, 541, 153

Gaskell, C.M., & Peterson, B.M. 1987, ApJS, 65, 1

Kataoka, J., et al. 2001, ApJ, 560, 659

Kirk, J., Rieger, F., & Mastichiadis, A. 1998, A&A, 333, 452

Koen, C. 1994, MNRAS, 268, 690

Litchfield, S.J., Robson, E.I., & Hughes, D.H. 1995, A&A, 300, 385

Maraschi, L., et al., 2002, in New visions of the X-ray Universe in the XMM-Newton and Chandra Era, ed. F. Jansen, in press (astro-ph/0202418)

Maoz, D., & Netzer, H. 1989, MNRAS, 236, 21

Peterson, B. M., Wanders, I., Horne, K., Collier, S., Alexander, T., Kaspi, S., & Maoz, D. 1998, PASP, 110, 660

Sembay, S., Edelson, R., Markowitz, A., Griffiths, R.G., & Turner, M.J.L. 2002, ApJ, 547, 634

Timmer, J., & König, M. 1995, A&A, 300, 707

Uttley, P., M^{c}Hardy, I.M., & Papadakis, I.E. 2002, MNRAS, 332, 231

Welsh, W.F. 1999, PASP, 111, 1347

White, R.J., & Peterson, B.M. 1994, PASP, 106, 879

Zhang, Y.H. 2002, MNRAS, 337, 609

Zhang, Y.H., et al. 1999, ApJ, 527, 719

Zhang, Y.H., et al. 2002, ApJ, 572, 762

Table 1. CCF analysis results of one pair of fake light curves(s)[a]

	Evenly sampled data			Periodically gapped data		
	$\tau_{\rm peak}$	$\tau_{\rm cent}$	$\tau_{\rm fit}$	$\tau_{\rm peak}$	$\tau_{\rm cent}$	$\tau_{\rm fit}$
ICCF	2900	3092	...	2600	2549	...
DCF	3072	3067	3020 ± 115	2018	2170	3483 ± 359
ZDCF	3072	3067	3030 ± 86	2018	2170	2993 ± 287

[a]The true lag is assumed to be 3000 s.

Table 2. CCPD analysis results of Monte Carlo simulation data (ks)[a]

True Lag	Evenly sampled data			Periodically gapped data		
	$\tau_{\rm peak}$	$\tau_{\rm cent}$	$\tau_{\rm fit}$	$\tau_{\rm peak}$	$\tau_{\rm cent}$	$\tau_{\rm fit}$
			ICCF			
0.00	$0.10^{+0.10}_{-0.30}$	$0.00^{+0.11}_{-0.10}$	...	$0.10^{+0.10}_{-0.30}$	$0.00^{+0.24}_{-0.24}$	...
0.30	$0.30^{+0.40}_{-0.10}$	$0.31^{+0.22}_{-0.20}$	...	$0.30^{+0.40}_{-0.10}$	$0.30^{+0.24}_{-0.25}$	...
1.40	$1.30^{+0.10}_{-0.10}$	$1.40^{+0.15}_{-0.14}$	...	$1.30^{+0.40}_{-0.10}$	$1.32^{+0.42}_{-0.35}$	...
3.00	$2.90^{+0.40}_{-0.10}$	$3.00^{+0.19}_{-0.19}$	...	$3.00^{+0.30}_{-0.30}$	$2.99^{+0.53}_{-0.47}$	...
5.40	$5.40^{+0.50}_{-0.10}$	$5.40^{+0.24}_{-0.24}$	...	$5.40^{+0.40}_{-0.10}$	$5.44^{+0.30}_{-0.32}$	...
7.10	$7.00^{+0.40}_{-0.10}$	$7.10^{+0.27}_{-0.24}$	...	$7.10^{+0.40}_{-0.10}$	$7.03^{+0.48}_{-0.38}$	...
			DCF			
0.00	$0.00^{+0.00}_{-0.00}$	$0.00^{+0.23}_{-0.23}$	$0.10^{+0.18}_{-0.16}$	$0.00^{+0.00}_{-0.00}$	$0.00^{+0.29}_{-0.07}$	$0.00^{+0.46}_{-0.44}$
0.30	$0.51^{+0.00}_{-0.00}$	$0.26^{+0.23}_{-0.02}$	$0.30^{+0.18}_{-0.17}$	$0.51^{+0.00}_{-0.51}$	$0.05^{+0.78}_{-0.05}$	$0.29^{+0.47}_{-0.45}$
1.40	$1.54^{+0.00}_{-0.00}$	$1.31^{+0.23}_{-0.02}$	$1.38^{+0.28}_{-0.23}$	$1.02^{+0.00}_{-0.00}$	$1.14^{+0.65}_{-0.45}$	$1.36^{+0.67}_{-0.62}$
3.00	$3.07^{+0.00}_{-0.00}$	$3.06^{+0.24}_{-0.24}$	$2.96^{+0.44}_{-0.38}$	$2.02^{+0.00}_{-0.00}$	$2.47^{+0.74}_{-0.41}$	$2.98^{+0.85}_{-0.79}$
5.40	$5.63^{+0.00}_{-0.51}$	$5.38^{+0.25}_{-0.24}$	$5.34^{+0.69}_{-0.64}$	$6.14^{+0.00}_{-1.54}$	$4.93^{+0.95}_{-0.72}$	$5.35^{+0.78}_{-0.62}$
7.10	$7.17^{+0.00}_{-0.00}$	$7.16^{+0.25}_{-0.24}$	$7.02^{+0.90}_{-0.81}$	$6.66^{+0.76}_{-0.00}$	$6.91^{+0.72}_{-0.93}$	$7.03^{+0.94}_{-0.82}$
			ZDCF			
0.00	$0.00^{+0.00}_{-0.00}$	$0.00^{+0.23}_{-0.23}$	$0.00^{+0.10}_{-0.10}$	$0.00^{+0.00}_{-0.00}$	$0.00^{+0.29}_{-0.07}$	$0.03^{+0.25}_{-0.23}$
0.30	$0.51^{+0.00}_{-0.00}$	$0.26^{+0.23}_{-0.02}$	$0.31^{+0.10}_{-0.10}$	$0.51^{+0.00}_{-0.51}$	$0.05^{+0.78}_{-0.05}$	$0.34^{+0.25}_{-0.25}$
1.40	$1.54^{+0.00}_{-0.00}$	$1.31^{+0.23}_{-0.02}$	$1.40^{+0.13}_{-0.12}$	$1.02^{+0.00}_{-0.00}$	$1.14^{+0.65}_{-0.45}$	$1.43^{+0.37}_{-0.38}$
3.00	$3.07^{+0.00}_{-0.00}$	$3.06^{+0.24}_{-0.24}$	$3.00^{+0.18}_{-0.19}$	$2.02^{+0.00}_{-0.00}$	$2.47^{+0.74}_{-0.41}$	$2.97^{+0.61}_{-0.54}$
5.40	$5.63^{+0.00}_{-0.51}$	$5.38^{+0.25}_{-0.24}$	$5.38^{+0.26}_{-0.32}$	$6.14^{+0.00}_{-1.54}$	$4.93^{+0.95}_{-0.72}$	$5.49^{+0.48}_{-0.39}$
7.10	$7.17^{+0.00}_{-0.00}$	$7.16^{+0.25}_{-0.24}$	$7.08^{+0.30}_{-0.41}$	$6.66^{+0.76}_{-0.00}$	$6.91^{+0.72}_{-0.93}$	$7.13^{+0.49}_{-0.47}$

[a]The quoted values are the medians of the CCPDs, and the errors are 68% confidence range with respect to the medians.

Table 3. CCF analysis results of the *XMM-Newton* data (s)

	Real data			Fake data		
	$\tau_{\rm peak}$	$\tau_{\rm cent}$	$\tau_{\rm fit}$	$\tau_{\rm peak}$	$\tau_{\rm cent}$	$\tau_{\rm fit}$
ICCF	300	1904	...	300	−212	...
DCF	0	100	695 ± 865	1200	707	1538 ± 2547
ZDCF	0	100	433 ± 179	1200	707	879 ± 592

Table 4. CCPD analysis results of the *XMM-Newton* data (s)[a]

	Real data			Fake data		
	$\tau_{\rm peak}$	$\tau_{\rm cent}$	$\tau_{\rm fit}$	$\tau_{\rm peak}$	$\tau_{\rm cent}$	$\tau_{\rm fit}$
ICCF	600^{+600}_{-600}	2021^{+867}_{-1092}	...	600^{+600}_{-1200}	1201^{+1617}_{-1541}	...
DCF	$0^{+0.600}_{-600}$	2011^{+881}_{-1104}	1279^{+566}_{-557}	1200^{+600}_{-1800}	1477^{+1101}_{-1110}	1767^{+777}_{-787}
ZDCF	$0^{+0.600}_{-600}$	2011^{+881}_{-1104}	712^{+418}_{-358}	1200^{+600}_{-1800}	1477^{+1101}_{-1110}	1457^{+716}_{-623}

[a]The quoted values are the medians of the CCPDs, and the errors are 68% confidence range with respect to the medians.

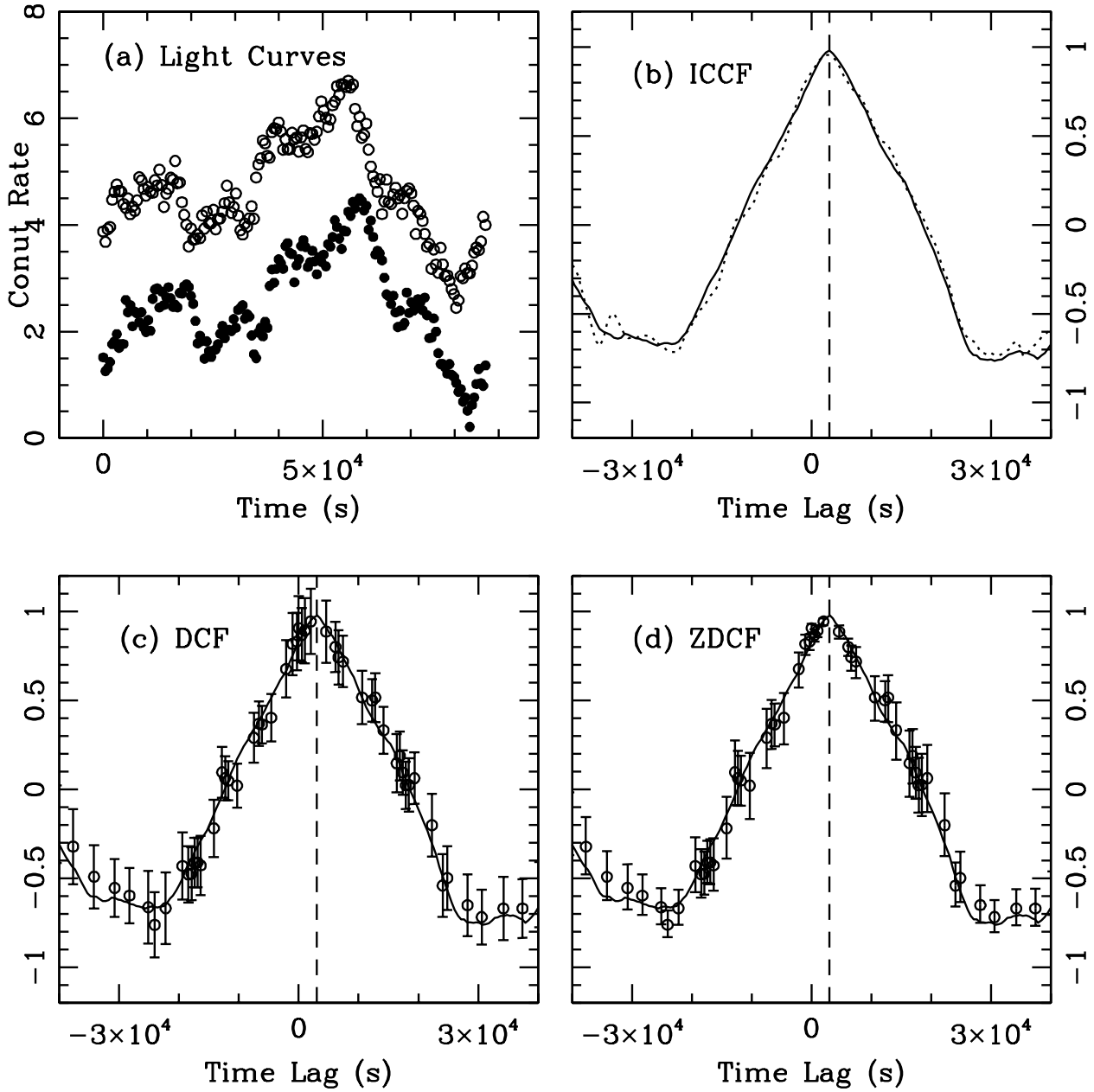

Fig. 1.— (a) An example of a fake light curve pair assuming τ = 3000 s between them. For clarity, the count rates of the second light curve (solid circles) are lowered by 1.5. (b) the corresponding ICCF of (a). The solid line is obtained from evenly sampled light curves, and the dashed line is obtained from periodically gapped light curves re-sampled from (a) after applying the real *BeppoSAX* observing windows; (c) the corresponding DCF of (a). The solid line is obtained from evenly sampled light curves, and the open circles with error bars are obtained from the same periodically gapped light curves as in (b); (d) same as (c), but for the ZDCF. The dashed lines in (b), (c) and (d) indicate the true lag.

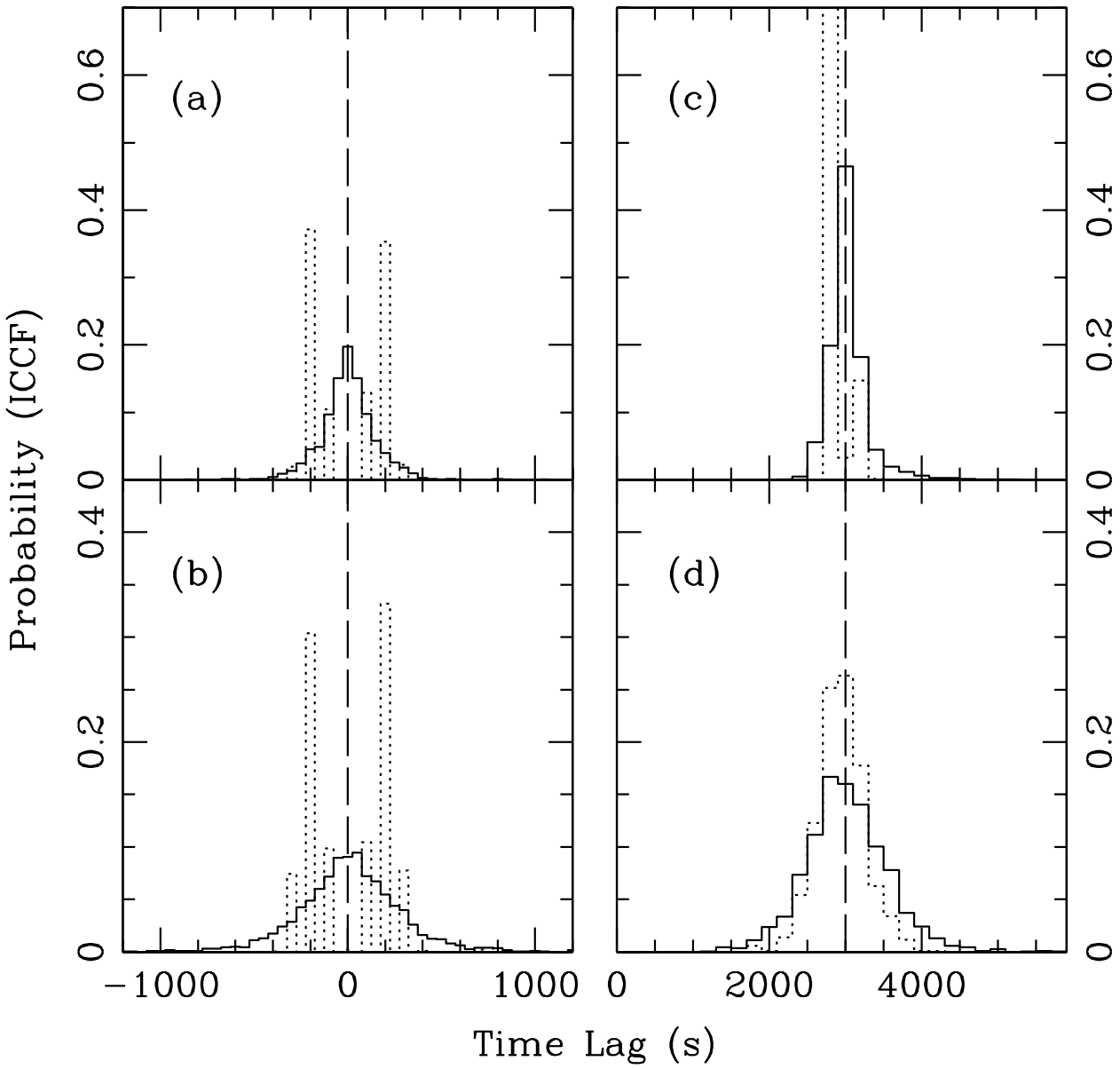

Fig. 2.— ICCF CCPDs for two different lags. (a) evenly sampled light curves with $\tau = 0$ s; (b) periodically gapped light curves with $\tau = 0$ s; (c) evenly sampled light curves with $\tau = 3000$ s; (d) periodically gapped light curves with $\tau = 3000$ s. The dotted line refers to $\tau_{\rm peak}$, and the solid line to $\tau_{\rm cent}$. The vertical long dashed line indicates the true lag.

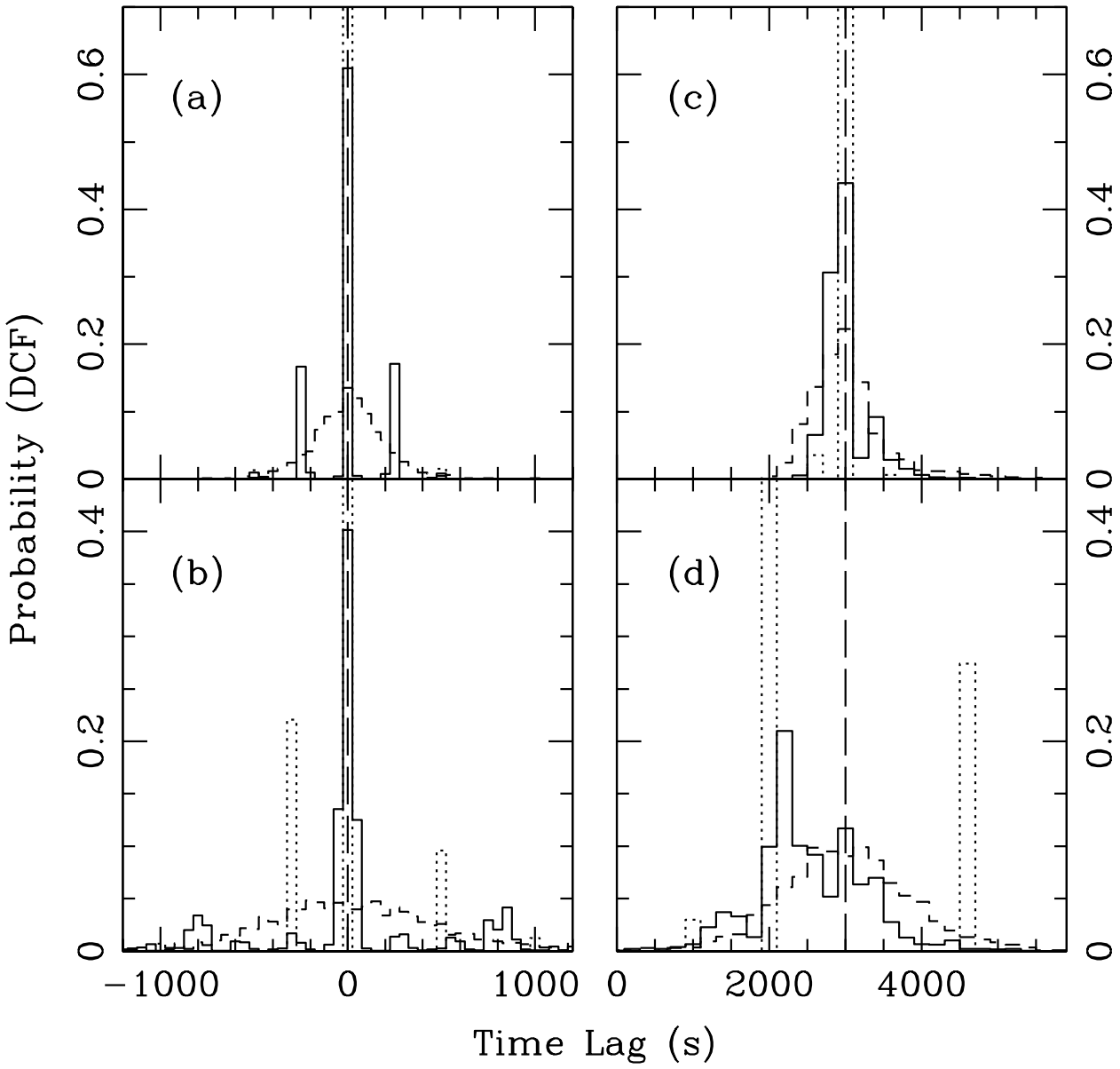

Fig. 3.— Same as Figure 2, but for DCF. The dotted line refers to $\tau_{\rm peak}$, the solid line to $\tau_{\rm cent}$, and the short dashed line to $\tau_{\rm fit}$. The vertical long dashed line indicates the true lag.

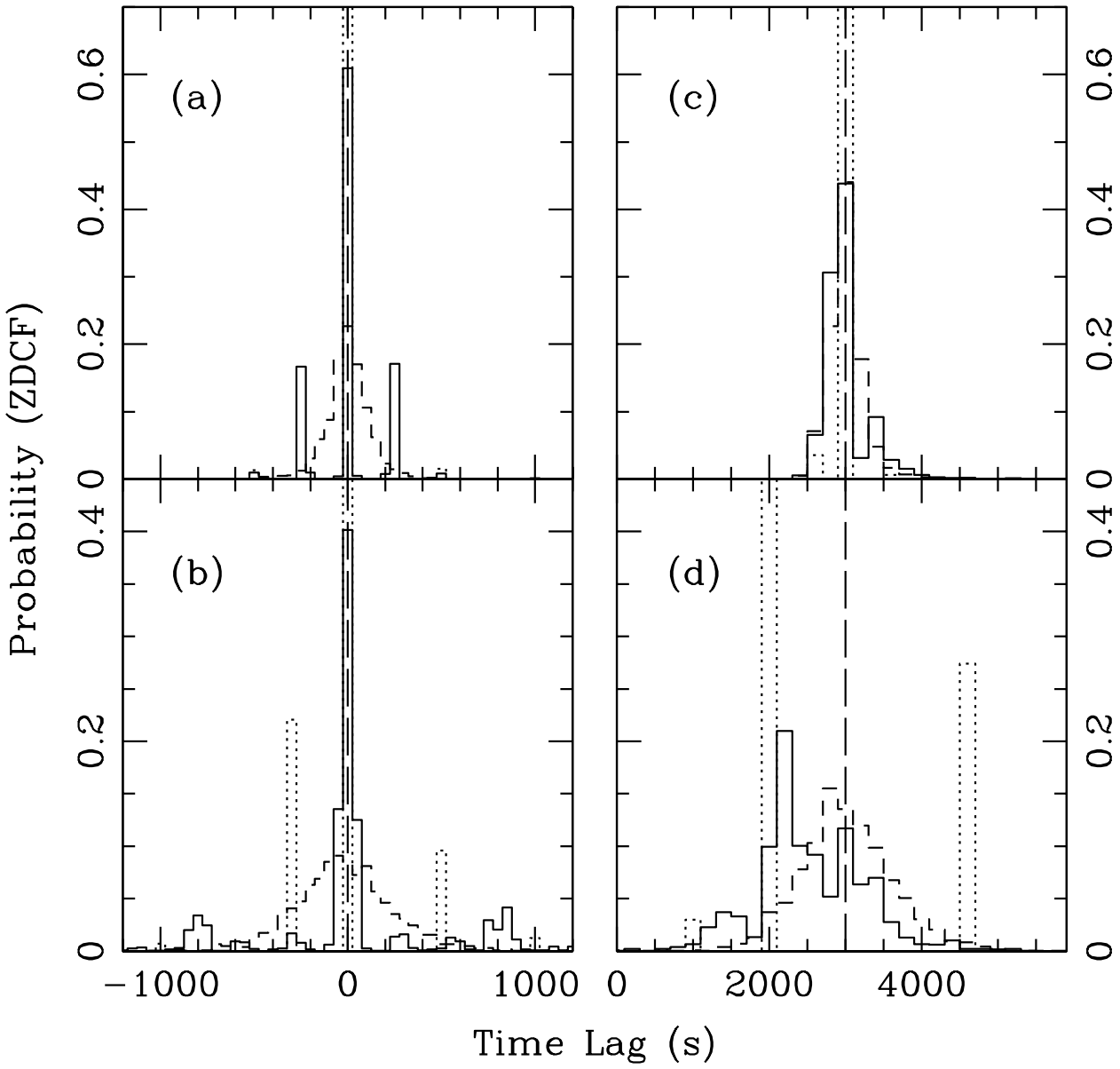

Fig. 4.— Same as Figure 2, but for ZDCF. The dotted line refers to $\tau_{\rm peak}$, the solid line to $\tau_{\rm cent}$, and the short dashed line to $\tau_{\rm fit}$. The vertical long dashed line indicates the true lag.

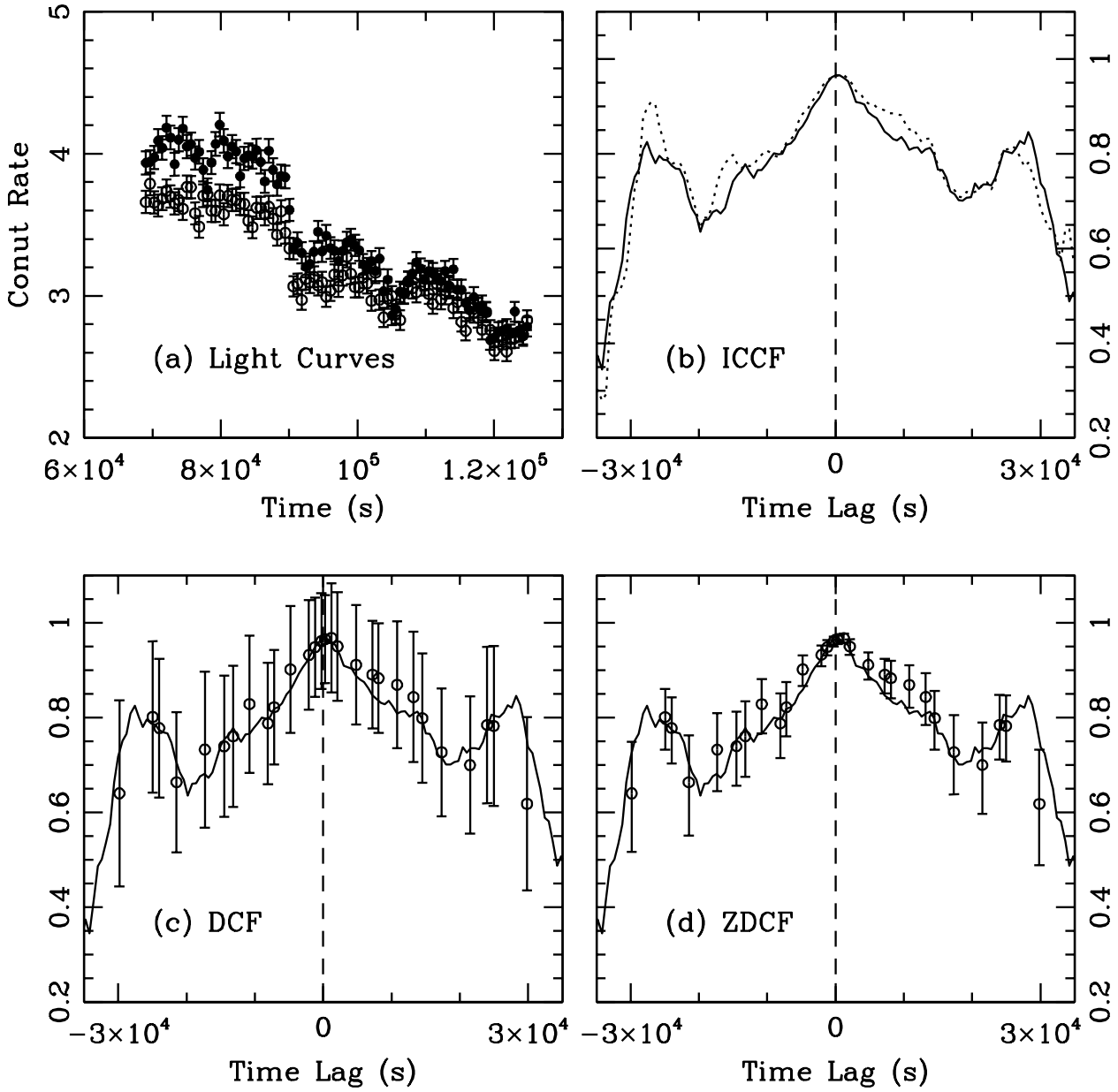

Fig. 5.— (a) A specific case: light curves obtained with *XMM-Newton* for PKS 2155–304 (see text for details). The solid circles refer to the 0.7–1 keV energy band, and the open ones to the 1–2 keV band. (b) the corresponding ICCF of (a). The solid line is calculated from real data (i.e., evenly sampled light curves), and the dashed line from periodically gapped light curves re-sampled from (a) after applying the *BeppoSAX* sampling windows to (a); (c) the corresponding DCF of (a). The solid line is calculated from real data, and the open circles with error bars from the same periodically gapped light curves as used in (b); (d) same as (c), but for ZDCF. The dashed lines in (b), (c) and (d) indicate zero lag.

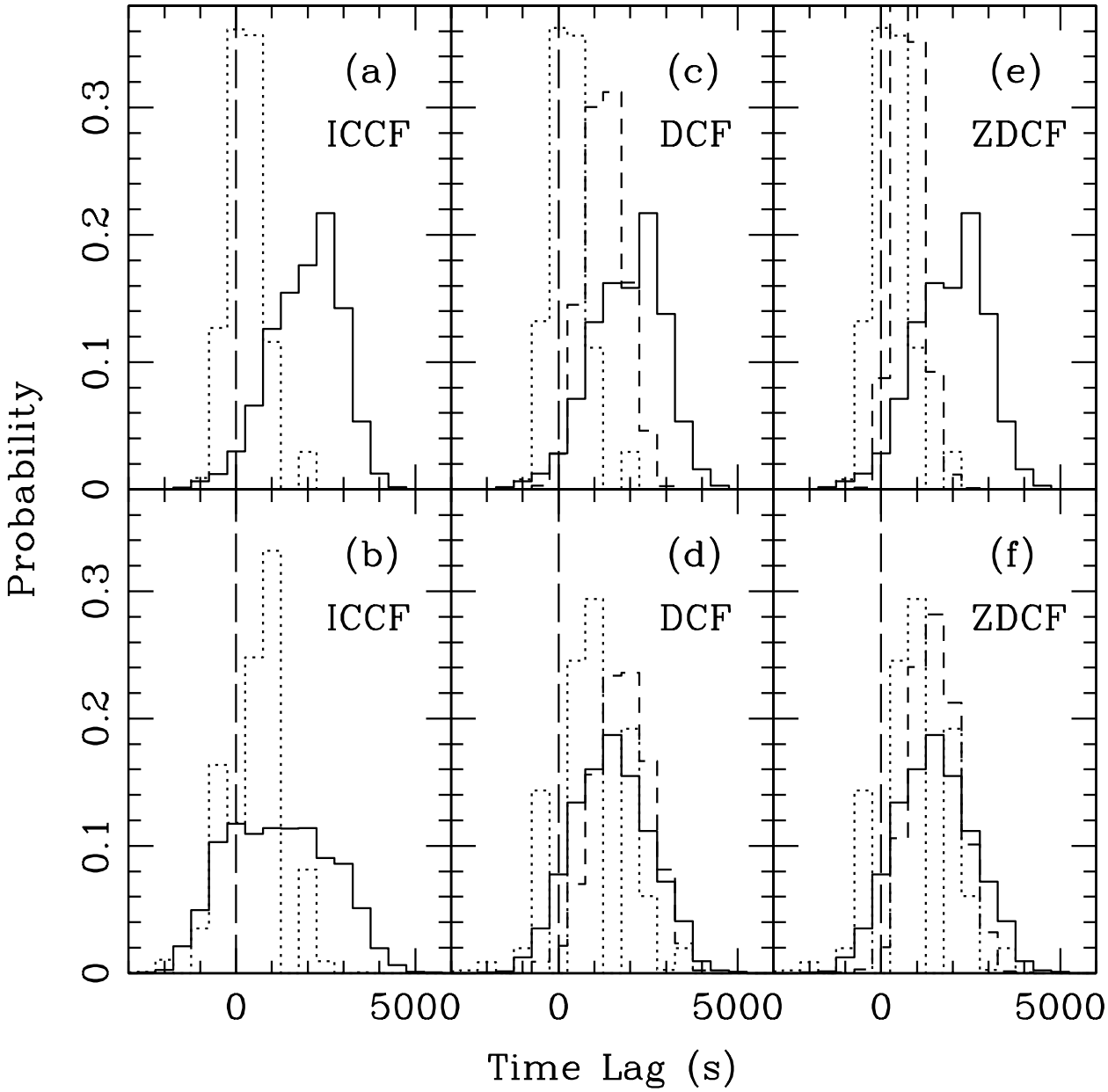

Fig. 6.— CCPDs obtained by Gaussian randomly redistributing the *XMM-Newton* light curves (Figure 5a) on the basis of the quoted errors. The upper panels are obtained from the real *XMM-Newton* light curves, and the lower panels from the periodically gapped light curves re-sampled from the real *XMM-Newton* light curves using the *BeppoSAX* sampling windows. The dotted line refers to $\tau_{\rm peak}$, the solid line to $\tau_{\rm cent}$, and the short dashed line to $\tau_{\rm fit}$. The vertical long dashed line indicates zero lag.